Available online at www.sciencedirect.com
ScienceDirect
Trans. Nonferrous Met. Soc. China 27(2017) 440−449
Transactions of Nonferrous Metals Society of China
www.tnmsc.cn

Sb(V) removal from copper electrorefining electrolyte: Comparative study by different sorbents

Katereh SALARI[1], Saeedeh HASHEMIAN[1], Mohammad Taghi BAEI[2]

1. Department of Chemistry, Islamic Azad University, Yazd Brunch, P. O. Box 89195-155, Yazd, Iran;
2. Department of Chemistry, Islamic Azad University, Azadshahr Branch, Azadshahr, P. O. Box 49617-89985 Golestan, Iran

Received 21 January 2016; accepted 9 April 2016

Abstract: Removal of Sb(V) from copper electrolyte by different sorbents such as activated carbon, bentonite, kaolin, resin, zeolite and white sand was investigated. Adsorption capacity of Sb(V) removal from copper electrolyte was as follows: white sand < anionic resin < zeolite < kaolin < activated carbon < bentonite. Bentonite was characterized using FTIR, XRF, XRD, SEM and BET methods. The results show specific surface area of 95 m^2/g and particles size of 175 nm for bentonite. The optimum conditions for the maximum removal of Sb are contact time 10 min, 4 g bentonite and temperature of 40 °C. The adsorption of Sb(V) on bentonite is followed by pseudo-second-order kinetic (R^2=0.996 and k=9×10^{-5} g/(mg·min)). Thermodynamic results reveal that the adsorption of Sb(V) onto bentonite from copper electrolyte is endothermic and spontaneous process (ΔG^{Θ}=−4806 kJ/(mol·K). The adsorption data fit both the Freundlich and Langmuir isotherm models. Bentonite has the maximum adsorption capacity of 10000 mg/g for adsorption of Sb(V) in copper electrolyte. The adsorption of Zn, Co, Cu and Bi that present in the copper electrolyte is very low and insignificant.

Key words: antimony (V); bentonite; copper electrolyte; sorbent; removal

1 Introduction

Antimony (Sb) is a toxic element. It is widely distributed in the lithosphere and has been widely applied in various industrial products such as increasing the hardness of alloys in lead–acid batteries and in small arms bullets, functioning as a flame retardant, being used in the clarification of glass products and metal electro refining [1,2]. High Sb concentrations in soil have been found at shooting ranges, mining and smelting areas and road sides [3]. Antimony is a co-impurity with copper in copper electrorefining electrolyte. The usual treatment has a number of disadvantages such as loss of high value copper in a low value recycle product. The production of copper from pyrometallurgical technologies leads to the production of an impure copper that is not of the purity required for most applications of the metal, thus, copper must be electrorefined [4]. Antimony exists in the environment in mainly two oxidation states: Sb(III) and Sb(V) [2]. While Sb(V) generally exists in oxidizing environments, Sb(III) dominates in reducing environments. Both Sb(III) and Sb(V) ions hydrolyze easily in aqueous solution, thus making it difficult to keep antimony ions stable in solution except in highly acidic media. Although Sb(III) compounds are 10 times more toxic than Sb(V) compounds, the mobility and solubility of Sb(V) are greater than Sb(III). Some studies showed that Sb(V) is the most stable form in environment [3,5].

A number of techniques have been developed for removing metal pollutant from aqueous effluents to minimize its impact. Although the traditional treatment methods such as precipitation, oxidation, reduction, electrochemical treatment, reverse osmosis, solvent extraction, adsorption, ion-exchange and evaporation can be used for the metal-bearing effluents, most of these methods are expensive and difficult to apply [6,7]. Among these methods, adsorption is an attractive process, in view of its efficiency and easiness [8]. Large numbers of experimental and modeling studies have been reported on the adsorption of cations, particularly heavy metal ions to pure earth components such as mineral clays. It is well-known that low-cost raw clay shows good adsorption properties [9].

Thus, a clear understanding of adsorption processes

Corresponding author: Saeedeh HASHEMIAN; Tel: +98-3531872572; Fax: +98-3537266560; E-mail: Sa_hashemian@iauyazd.ac.ir
DOI: 10.1016/S1003-6326(17)60050-5

is important in determining the transformation and fate of antimony in the aquatic system. The sorption behaviors of Sb(V) and Sb(III) on hydroxides of Fe, Mn, Al, humic acids, and mineral clays were studied [5,10].

Removal of Sb by different methods such as Fe−Mn binary oxide [11] and coagulation−flocculation−sedimentation was studied [12]. Role of trivalent antimony in the removal of As, Sb, and Bi impurities from copper electrolytes was studied [13]. Only very small number of adsorption studies of Sb on natural sorbents has been reported to date. Mineral clays such as bentonite and kaolin are widely used as catalysts, adsorbents and nano composites [14−16]. The adsorption of metal ions by kaolin was studied [17,18]. The use of clays for the adsorption or removal of heavy metals in wastewater has recently been the object of study in many researches due to innumerous economical advantages [19,20]. The cost of clays is relatively low in comparison to other alternative adsorbents. Clays and minerals such as montmorillonite, vermiculite, illite, kaolinite and bentonite are among those natural materials which have been investigated as heavy metal adsorbents. Another advantage of using clay as adsorbent resides in its intrinsic properties, such as high specific surface area, excellent physical and chemical stability, and several other structural and surface properties [21].

Bentonites are clay-rich in smectite regardless of their origin [22], which are valued for their properties such as crystal shape and size, cation exchange capacity (CEC), hydration and swelling, thixotropy, bonding capacity, impermeability, plasticity and tendency to react with organic and inorganic compounds [23,24]. The Gaomiaozi (GMZ) bentonite and nano-MoS_2/bentonite composite were used as sorbent [25,26].

Surface adsorption technique is the most widely used for Sb removal [27]. Removal of antimonite (Sb(III)) and antimonate (Sb(V)) from aqueous solution was studied using carbon nanofibers [28], Fe-modified aerobic granules [29], goethite [30] and perlite [31]. Role of Sb(V) in removal of As, Sb and Bi impurities from copper electrolyte was investigated [32].

In the present study, the application of different sorbents such as activated carbon, bentonite, kaolin, white sand, resin and zeolite adsorption for removal of antimony impurities from a Iranian (Kerman) copper electrorefining solution was studied. Different variables of the adsorption process were discussed.

2 Experimental

Activated carbon, zeolite and other chemicals were obtained from Merck. White sand was obtained from local mine of Kerman(Sharbabak). The raw kaolin and bentonite were obtained from local mine of Yazd (Iran). The chemical compositions of bentonite from XRF results are shown in Table 1. The raw bentonite was crushed and passed through a 150 μm sieve and baked at 350 °C. The specific surface area of the bentonite was determined as 95 m^2/g by BET method using N_2 adsorption. The experiments were carried out using a fresh electrolyte solution, with composition of 46.7 g/L Cu(II), 6.4 g/L As, 336. 25 mg/L Sb(V) and 160 g/L H_2SO_4 at the Kerman−Sarcheshmeh copper electro-refining. The concentrations of Ni, Zn, As, Pb, Fe, ions in copper electrolytes were 378 mg/L, 230 mg/L, 6.44 g/L, 11.00 mg/L and 1.92 mg/L, respectively. The density (ρ) of electrolyte was 1.196 g/L.

Table 1 Chemical compositions of bentonite from XRF analysis (mass fraction, %)

SiO_2	Al_2O_2	MgO	Fe_2O_2	CaO
76.84	9.11	2	1.34	1.4
Na_2O	K_2O	TiO_2	LOI	SO_3
2.52	1.38	0.23	2.86	2.19

The adsorption experiments were conducted in a 0.5 L glass vessel (included 40 mL of electrolyte and 4 g sorbent), which was stirred mechanically at 100 r/min.

All chemicals used were of analytical grade and without further purification. Double distilled water was used throughout. All samples were analyzed within 2 d of completing each test. All experiments were performed in duplicate.

IR measurements were performed by FTIR tensor-27 of Burker Co., using the KBr pellet. The powder X-ray diffraction studies were made on Philips PW3719 X-ray diffractometer by using Cu K_α radiation of wave length 1.54060 Å. All pH measurements were carried out with WTW pH 323. The morphology of bentonite was characterized by transmission electron microscopy (TEM Philips-CM). The nitrogen adsorption/desorption isotherm was measured by Quanta chrome, Autosorb-1.

The concentrations of Sb were measured using Varian double beam flame atomic absorption spectrophotometer (Varian AA−975, AA−1275).

The removal rate (η) of Sb by the hereby adsorbent is given by

$$\eta = (\rho_0-\rho_e)/\ \rho_0\times 100\% \quad (1)$$

where ρ_0 and ρ_e denote the initial and equilibrium concentrations (mg/L) of Sb, respectively. The amount of Sb adsorbed (q_e) was determined by

$$q_e = \frac{(\rho_0-\rho_e)V}{m} \quad (2)$$

where V is the volume of the solutions (mL) and m is the mass (g) of adsorbent.

3 Results and discussion

3.1 Effect of different sorbents on Sb(V) removal from copper electrolyte

For removal of Sb from copper electrolyte, different sorbents such as bentonite, kaolin, white sand, resin, zeolite and activated carbon were investigated. For adsorption study, at each of experiments, both of Sb and Cu concentrations were determined. The results are shown in Fig. 1. It is very important in the adsorption process of copper electrolyte that only Sb removal occurred and the concentration of copper in the electrolyte was not reduced. Results from Fig. 1 show that bentonite and activated carbon have the most adsorption efficiency for Sb removal from copper electrolyte. The removal rates of Sb onto bentonite and activated carbon were 68% and 67%, respectively, but copper removal only was 2% for both of adsorbents. It was found that the adsorption rate of Sb reaches a maximum of 48% onto kaolin. The results showed that the adsorption capacity of Sb(V) removal from electrorefining electrolyte is as follows: white sand < anionic resin < zeolite < kaolin < activated carbon < bentonite.

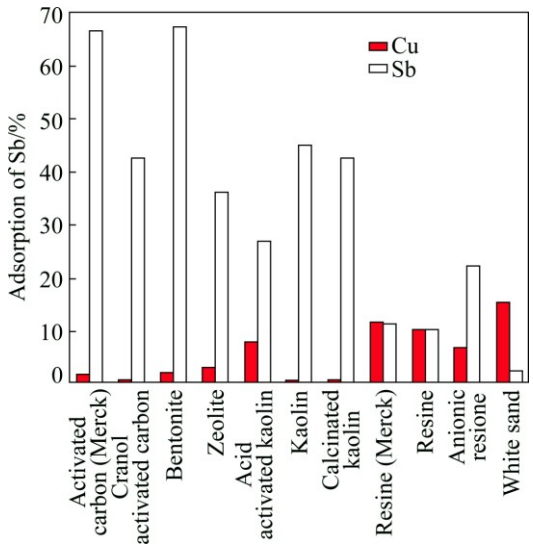

Fig. 1 Effect of different sorbents for adsorption of Sb(V) from copper electrolyte

Activated carbon is widely used as an adsorbent due to its high surface area and high adsorption capacity, but activated carbon is not economically viable and technically efficient [33,34]. The use of low-cost, locally available, biodegradable substitutes made from natural sources has been explored for the removal of pollutant from industrial effluent [35−40]. Natural clays are low-cost, readily available, and excellent adsorbents [36]. For these reasons, bentonite was chosen as the selective and the best sorbent for Sb removal from copper electrolyte. It is important that the bentonite did not remove the copper from electrolyte.

As it is well known, the mineral clays are hydrous aluminium silicate and are classified as phyllosilicates. They have a layered structure which can be described as constructed from two modular units: a sheet of cornerlinked tetrahedra and a sheet of edge-linked octahedra. Each tetrahedron consists of M^{x+} cation, coordinated to four oxygen atoms, and linked to adjacent tetrahedra by sharing three corners [41]. The dominant M^{x+} cation in the tetrahedral sheet is Si^{4+}, but Al^{3+} substitutes it frequently and Fe^{3+} occasionally. The octahedral sheet can be thought of as two planes of closed-packed oxygen ions with cations occupying the resulting octahedral sites between two planes. Therefore, Sb(V) ions were adsorbed strongly on the negative charges on the surface of bentonite (Fig. 2).

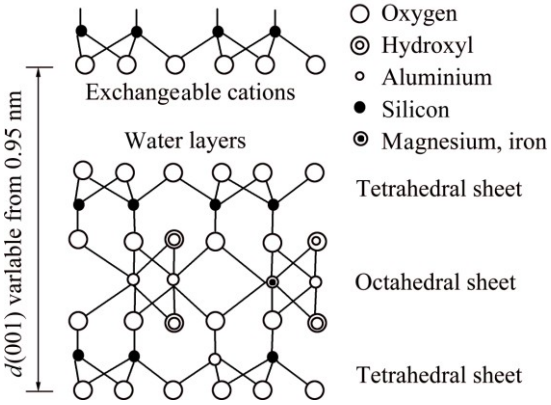

Fig. 2 Chemical structure of bentonite

3. 2 Characterization of bentonite

FTIR of bentonite is shown in Fig. 3. The broad band at 3439 cm^{-1} corresponding to stretching vibration of OH groups is attached to octahedral layer of bentonite. The Si—O stretching band at 1641 cm, the Si—O—Si asymmetric stretching band at 1001 cm and the Si—O—Al bending band at 668 cm are clearly seen. From FTIR of bentonite (Fig. 3), the Si—O stretching vibrations were observed at 831, 668, 475 and 1001 cm showing the presence of quartz [42]. FTIR of bentonite adsorbed 200 mg/L Sb(V) solution is also shown in Fig. 3(c). The bentonite adsorbed copper electrolyte in Fig. 3(b) also confirms the adsorption of Sb from electrolyte by bentonite. The peak of 3439 cm is just about weak and disappeared for bentonite adsorbed copper electrolyte. For bentonite adsorbed 200 mg/L Sb, this band shifts to sharp band at 3326 cm. The small peaks appeared at 2357 and 2224 cm. The sharp peak of 1702 cm^{-1} also becomes visible.

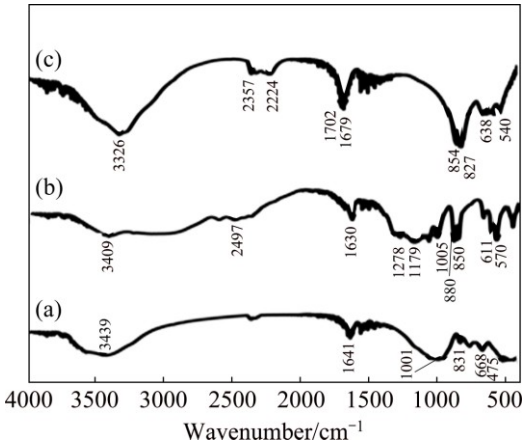

Fig. 3 FTIR of bentonite (a), bentonite adsorbed electrolyte (b), bentonite adsorbed 200 mg/L Sb (c)

The XRD pattern of bentonite is given in Fig. 4. The XRD pattern of bentonite indicates the sharp and intense peak attributed on crystalline quartz (2θ=27°). The small peaks at 2θ=6°, 21° and 35° are attributed to montmorillonite. The XRD analysis of bentonite is shown in Table 2. The results show that phases of quartz, montmorillonite, anhydrite and orthoclase are seen in the bentonite and the main phases of bentonite are quartz and montmorillonite. EDAX analyses are as follows: 27.89% Si, 13.39% Al, 0.26% Ti, 2.5% Fe, 1.86% Ca, 1.35% Mg and 0.25% K (mass fraction).

SEM image of bentonite is shown in Fig. 5. The image shows the particle size of about 175 nm for bentonite after calcination at 500 °C.

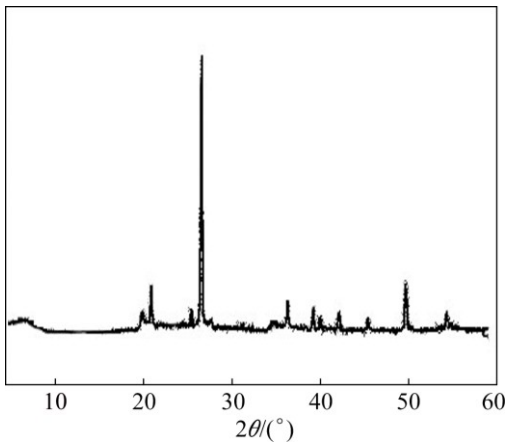

Fig. 4 XRD pattern of bentonite

Table 2 XRD analysis of bentonite

Compound	Formula	Mass fraction/%
Quartz	SiO_2	56
Anhydrite	$CaSO_4$	4
Orthclase	$KAlSi_3O_8$	4
Montmorillonite	$Ca_{0.2}(Al,Mg)_2$-$Si_4O_{10}(OH)_2{\cdot}xH_2O$	35

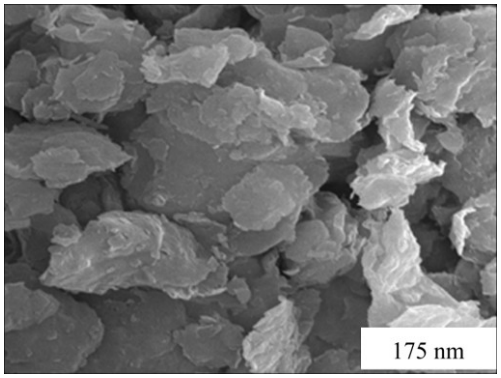

Fig. 5 SEM image of bentonite calcinated at 500 °C

The N_2 adsorption–desorption isotherm of bentonite is presented in Fig. 6. Bentonite has surface area of 95 m^2/g, pore volume 0.156 cm^3/g and pore diameter 100 nm. The isotherm is between types IV and II, which is the characteristic of porous structures. The hysteresis loop, which is very common in this type of clays [42], is associated with network effects of N_2 desorption from the house of cards structure, indicating the random orientation of layers. These results show the layered and porous structures of bentonite and it acts as a suitable sorbent for removal of Sb.

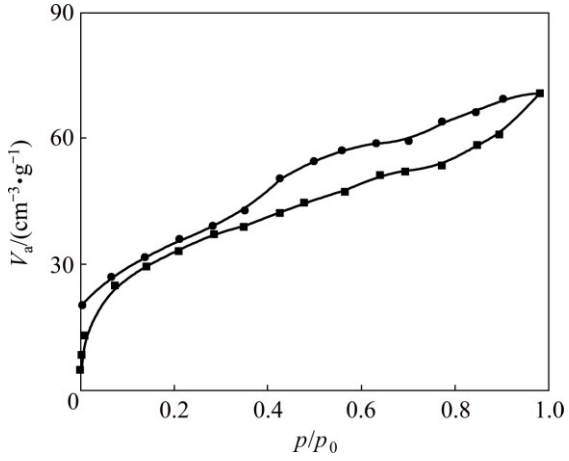

Fig. 6 N_2 adsorption–desorption isotherms of bentonite

3.3 Adsorption study

3.3.1 Effect of contact time

The effect of contact time on the adsorption of Sb(V) ions by bentonite is shown in Fig. 7. The removal of Sb(V) ions increased rapidly with time up to 10 min and thereafter increased slowly. The uptake of Sb(V) ions was 50.0%, 68.4% and 72.0% at 10 min, 60 min and 120 min, respectively. According to the results, the equilibrium reached at 60 min and was taken as the optimal contact time for the subsequent experiments. It is very important that after 60 min of contact time of electrolyte by bentonite, the Cu removal rate is less than 4% and very insignificant. Therefore, the concentration of Cu in the electrolyte after adsorption process does not decrease.

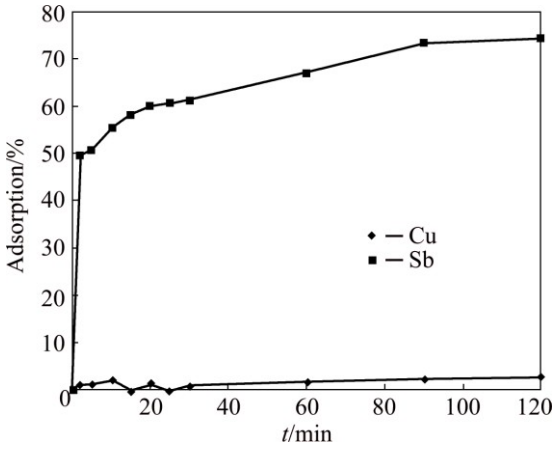

Fig. 7 Effect of contact time on removal of Sb by bentonite from copper electrolyte

3.3.2 Effect of pH

The effect of pH on Sb(V) adsorption by bentonite is shown in Fig. 8. It is well known that adsorption of metal ions depends on pH of aqueous solution.

The adsorption of Sb(V) onto bentonite is strongly dependent on pH. At pH 2.5, the amount of adsorbed Sb(V) on bentonite remained more than 95%, while the amount of adsorbed Sb(V) on bentonite reduced to 30% at pH>2.6. The similar pH-dependence of Sb(V) adsorption on iron oxide has been reported [43,44].

In this study, the pH of copper electrolyte was 0. The uptake of Sb at this pH was almost 70%, but no Cu removal was observed at pH 0. Therefore, the same pH of electrolyte (pH 0) is suitable for Sb removal.

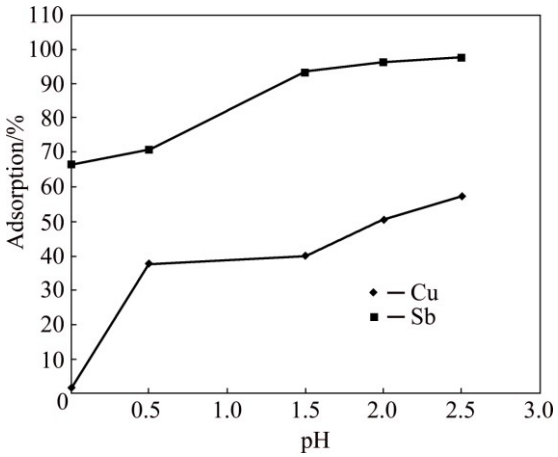

Fig. 8 Effect of pH on adsorption of removal of Sb by bentonite from copper electrolyte

3.3.3 Effect of amount of bentonite

Adsorbent dosage is an important parameter for adsorption. The adsorption of Sb(V) on bentonite from copper electrolyte was studied by changing the amount of bentonite (0.4−4.4 g, 40 mL) at contact time for 60 min (Fig. 9). The results are shown in Fig. 9. Figure 9 indicates that, with increasing dosage of bentonite, the adsorption rate increased. The adsorption rate increased from 22.4% to 68%, as the bentonite dose increased from 0.4 g to 4.4 g(40 mL) at equilibrium time (60 min). This is due to some of adsorption sites remaining unsaturated during the adsorption reaction [45]. The results also showed the removal of copper from electrolyte which was very little and neglectable.

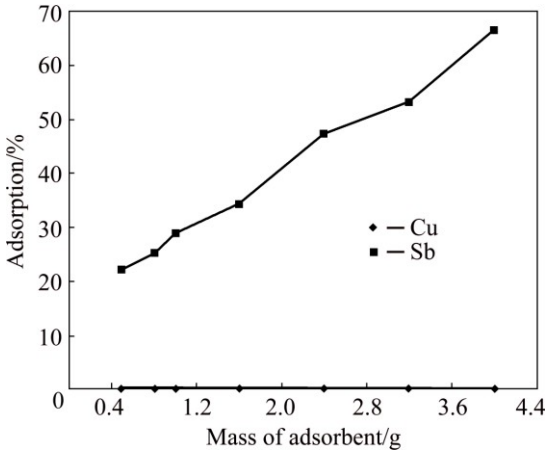

Fig. 9 Effect of mass of bentonite on adsorption of Sb from copper electrolyte

3.3.4 Effect of temperature

In order to evaluate the effect of temperature on the removal of Sb from electrolyte, the adsorption experiments were conducted in the temperature range of 25−65 °C. The results showed that with increasing temperature to 40 °C, the adsorption capacity of Sb onto bentonite was increased (Fig. 10). It looks due to more interaction of Sb ions and sorbent at higher temperatures. Removal rate of Sb for temperature of more than 40 °C was not observed. The increasing of adsorption with rise in temperature indicates that the adsorption process in the present case is endothermic and adsorption reaction of Sb(V) on bentonite absorbs energy.

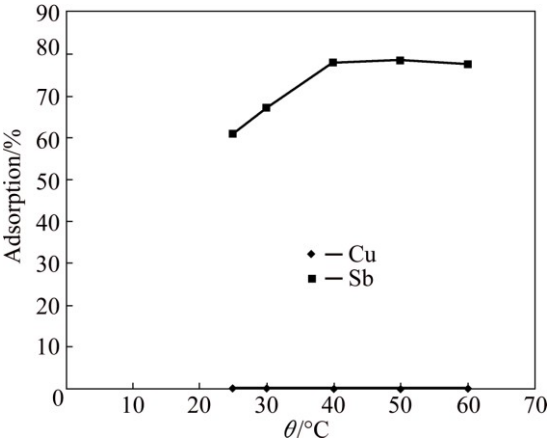

Fig. 10 Effect of temperature on adsorption of Sb onto bentonite

3.4 Kinetic of adsorption

One of the most important features of the adsorbent material is the rate with which the solid phase adsorbs metal ions from the aqueous solutions and attains equilibrium. In order to investigate the adsorption kinetics of Sb onto bentonite, pseudo-first-order and pseudo-second-order models have been investigated. The conformity between experimental data and the model predicted values was expressed by the correlation coefficients (R^2, values close or equal to 1). The relatively higher value is the more applicable model to the kinetics of Sb removal.

The pseudo-first-order equation is generally expressed as follows:

$$\mathrm{d}q_t/\mathrm{d}t=k_1(q_e-q_t) \quad (3)$$

The linear equation for the pseudo-first-order of the kinetic model is expressed as [46]

$$\ln(q_e-q_t)=\ln(q_e)-k_1t \quad (4)$$

where q_e and q_t are the adsorption capacities at equilibrium and at time t, respectively (mg/g), k_1 is the rate constant of the pseudo-first order adsorption (min^{-1}). In order to obtain the rate constant, the values of $\ln(q_e-q_t)$ were linearly correlated with t by plotting $\ln(q_e-q_t)$ versus t to give a linear relationship from which k_1 and predicted q_e can be determined from the slope and intercept of the plot, respectively (Fig. 11).

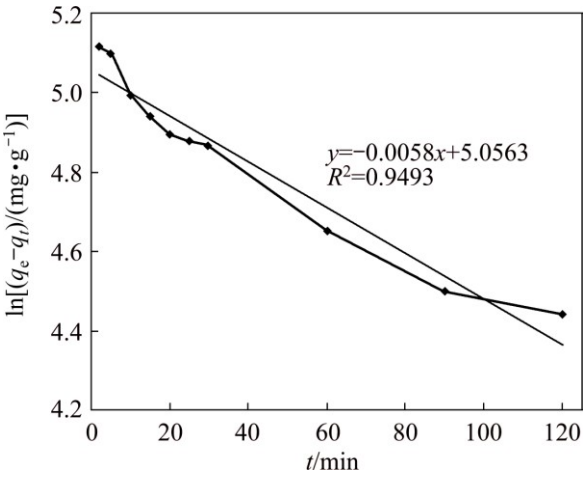

Fig. 11 Pseudo-first order kinetics for adsorption of Sb by bentonite from copper electrolyte

The adsorption kinetic may be described by the pseudo-second order model [47]. The differential equation is generally given as follows:

$$t/q_t=t/q_e+1/(k_2q_e^2) \quad (5)$$

where k_2 ($\mathrm{g/(mg^{-1}\cdot min^{-1})}$) is the second-order rate constant of adsorption. If the second-order kinetic is applicable, then the plot of t/q_t versus t should show a linear relationship. Value of k_2 and equilibrium adsorption capacity q_e were calculated from the intercept and slope of the plot of t/q_t versus t (Fig. 12). The linear plot of t/q_t versus t shows good agreement with the experiment.

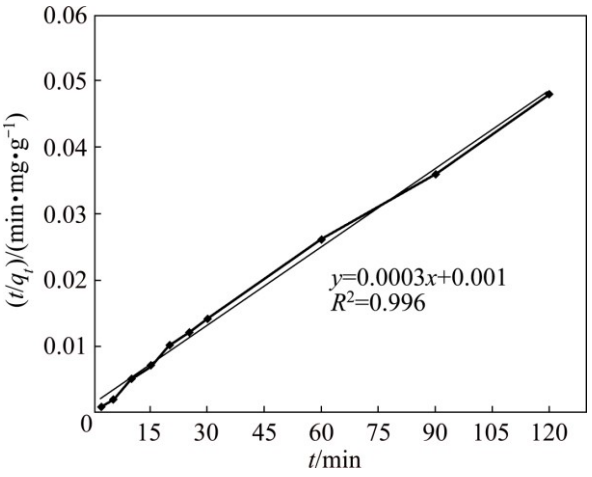

Fig. 12 Pseudo-second order kinetics for adsorption of Sb by bentonite from copper electrolyte

The first order kinetic model has rate constant of 5.8×10^{-3} $\mathrm{min^{-1}}$ and R^2 of 0.949. The correlation coefficient for the second-order kinetic model is 0.996, which led to believe that the pseudo second-order kinetic model provided good correlation for the adsorption of Sb onto bentonite from electrorefining electrolyte ($k_2=9.0\times10^{-5}$ $\mathrm{g/(mg^{-1}\cdot min^{-1})}$).

3.5 Thermodynamic parameters

The adsorption of Sb(V) onto bentonite was investigated at different temperatures (25−50 °C). Various thermodynamic parameters such as free energy change, entropy change and enthalpy change of Sb adsorption were calculated. The standard enthalpy (ΔH^{Θ}) and standard entropy changes (ΔS^{Θ}) can be calculated from the slope and intercept of the plot of $\ln K$ versus $1/T$ (Fig. 13) by

$$\ln K=\Delta S^{\Theta}/R+\Delta H^{\Theta}/(RT) \quad (6)$$

The Gibbs free energy (ΔG^{Θ}) of adsorption can be calculated by

$$\Delta G^{\Theta}=\Delta H^{\Theta}-T\Delta S^{\Theta} \quad (7)$$

The value of ΔG^{Θ} was consequently calculated by

$$\Delta G^{\Theta}=-RT\ln K_c \quad (8)$$

where R is the gas mole constant (8.3145 J/(mol·K)), K_c is the equilibrium constant and T is the temperature in K. Thermodynamic parameters for adsorption of Sb(V) by bentonite from copper electrolyte are shown in Table 3.

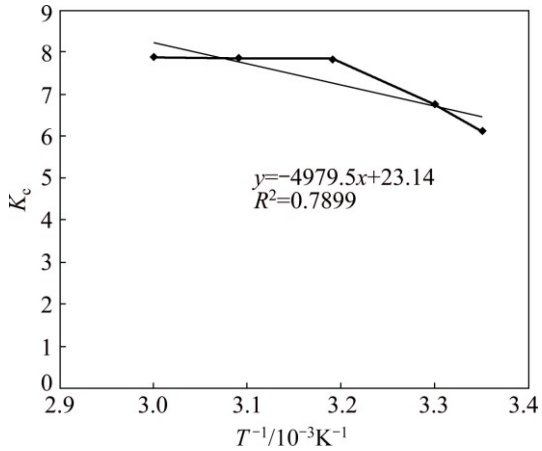

Fig. 13 Plot of ln K_c verses 1/T

Table 3 Thermodynamic parameters for adsorption of Sb by bentonite from copper electrolyte

ΔS^{Θ}/ (J·mol^{-1}·K^{-1})	ΔH^{Θ}/ (kJ·mol^{-1})	ΔG^{Θ}/ (kJ·mol^{-1})	K_c	T/K
		−4806	6.10	298
		−5013	6.74	303
192.4	41.4	−5334	7.81	313
		−5532	7.84	323
		−5711	7.88	333

3.6 Adsorption isotherms

The relationship between the amount of a substance adsorbed at constant temperature and its concentration in the equilibrium solution is called the adsorption isotherm. The adsorption isotherm is important from theoretical and practical point of view. Equilibrium isotherm equations are used to describe the experimental sorption data. The parameters obtained from the different models provide important information on the sorption mechanisms and the surface properties and affinities of the sorbent. The most widely accepted surface adsorption models for single-solute systems are the Langmuir and Freundlich models. Linear regression is frequently used to determine the best-fitting isotherm, and the applicability of isotherm equations is compared by judging the correlation coefficients. Freundlich and Langmuir models were used to fit the experimental data. The linearized forms of Langmuir and Freundlich equations for the adsorption data are shown in Figs. 14 and 15, respectively. The Langmuir isotherm assumes a surface with homogeneous binding sites, equivalent sorption energies, and no interaction between adsorbed species. Its mathematical form is written as

$$\rho_e/q_e=(1/q_{max}K_L)+\ \rho_e/q_{max} \quad (9)$$

where q_{max} and K_L represent the maximum adsorption capacity for the solid phase loading and the energy constant related to the heat of adsorption respectively (Fig. 14). A plot of ρ_e/q_e versus ρ_e gives K_L and q_{max} if the isotherm follows the Langmuir equation.

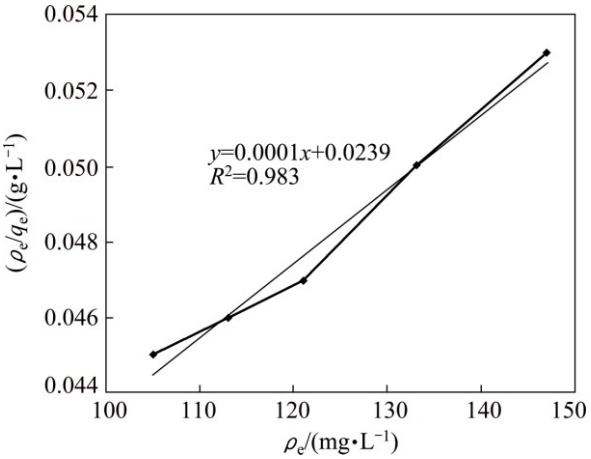

Fig. 14 Langmuir isotherm for adsorption of Sb by bentonite from copper electrolyte

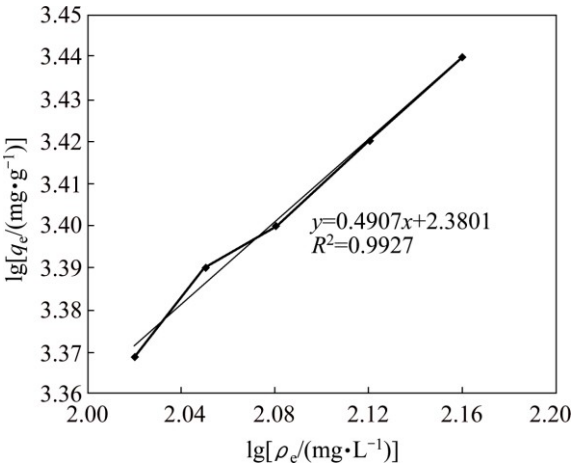

Fig. 15 Freundlich isotherm for adsorption of Sb by bentonite from copper electrolyte

The dimensionless parameters of the equilibrium or adsorption intensity, R_L, based on the further analysis of Langmuir equation can be expressed as

$$R_L=\frac{1}{1+b\rho_e} \quad (10)$$

There are four probabilities for the R_L value: 1) for favorable adsorption, $0<R_L<1$; 2) for unfavorable adsorption, $R_L>1$; 3) for linear adsorption, $R_L=1$; and 4) for irreversible adsorption. Favorable adsorption value of R_L (9.8×10^{-6}) was observed from Table 4.

Table 4 Langmuir and Freundlich isotherm parameters for adsorption of Sb onto bentonite from copper electrolyte

Freundlich				Langmuir		
K_F/ (L·mg^{-1})	n	R^2	q_{max}/ (mg·g^{-1})	K_L/ (L·mg^{-1})	R^2	R_L
251.1	2.1	0.992	10000	239	0.983	9.8×10^{-6}

The Freundlich isotherm is an empirical equation based on

$$q_e=K_F\rho_e^{1/n} \quad (11)$$

$$\lg q_e=\lg K_F+1/n \lg \rho_e \quad (12)$$

where K_F (L/g) and n are Freundlich constants related to adsorption capacity and adsorption intensity, respectively (Fig. 15). The intercept K_F obtained from the plot of lg q_e versus ln ρ_e is roughly a measure of the sorption capacity and the slope (1/n) of the sorption intensity (Table 4). It was indicated by that magnitude of the term (1/n) gives an indication of the favorability and capacity of the adsorbent/adsorbate systems [48].

3.7 Industrial experiments

Industry experiments for adsorption of Sb onto bentonite from copper electrolyte for different ratios of electrolyte to bentonite were studied. The results are shown in Fig. 16. The results show that the ratio of 8% Sb to bentonite has the highest efficiency for adsorption of Sb from 20 L of copper electrolyte. It showed more than 80% Sb removal occurred after 30 min of contact time, without removing the copper from electrolyte.

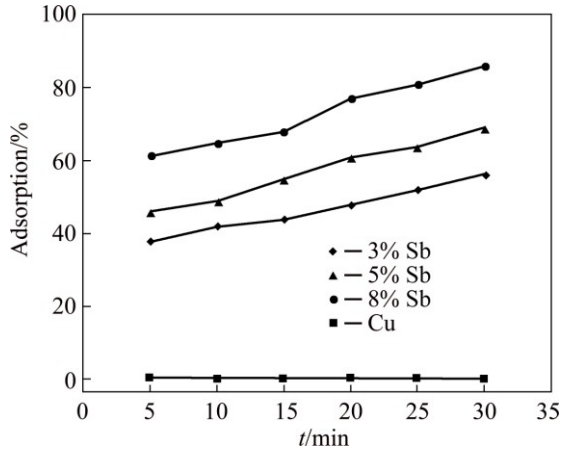

Fig. 16 Industrial experiments for adsorption of Sb onto bentonite from copper electrolyte at different ratios of electrolyte to bentonite

Finally, the adsorption of cations such as Ni, Zn, As, Pb, Fe, Co and Bi in the copper electrolyte were investigated. 20 L of copper electrolyte with 2 kg of bentonite was examined at 30, 60 and 120 min. Figure 17 shows the adsorption of co-contaminants cations with copper electrorefining electrolyte. It is obvious that the adsorption of Zn, Co, Cu and Bi is very low and insignificant. The content of Fe ion was increased after adsorption by bentonite from copper electrorefining electrolyte. The Sb and Pb ions were adsorbed in high efficiency, therefore, the adsorption of Sb and Pb was also considerable.

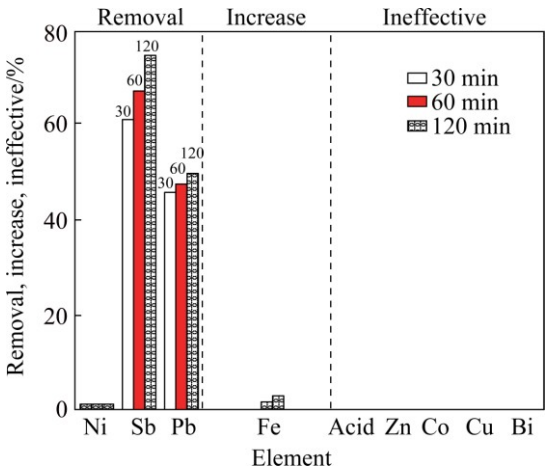

Fig. 17 Adsorption of other metal ions in copper electrorefining electrolyte by bentonite

4 Conclusions

The adsorption of Sb(V) from copper electrolyte onto different sorbents such as activated carbon, bentonite, kaoline, resin, zeolite and white sand were examined. Among these sorbents, bentonite had the best adsorption capacity for Sb from copper electrorefining electrolyte. Therefore, the adsorption of Sb(V) by bentonite was discussed in this study. The effects of contact time, pH, mass of bentonite and temperature were examined. The adsorption of Sb(V) on bentonite reached equilibration within 60 min. Adsorption of Sb onto bentonite can be used for separating this impurity from copper electrolyte and recycling the electrolyte to the electrorefining cells. The results indicate that the adsorption kinetics follows the pseudo-second-order model. The thermodynamic parameters of the adsorption of Sb were calculated and negative values of the free energy change indicate that the adsorption is spontaneous. The extent of Sb removal can be enhanced using a greater bentonite to solution ratio. The adsorption of Sb onto bentonite did not change the concentration of Zn, Co, Cu and Bi ions, but decreased the adsorption of Sb and Pb from copper electrolytes.

Acknowledgements

The authors thank from Kerman-Sarcheshmeh copper electrorefining (Iran) and Islamic Azad University, Yazd Brunch for support to carry out this work.

References

[1] FILELLA M, BELZILE N, CHEN Y W. Antimony in the environment: A review focused on natural waters [J]. Earth-Science Reviews, 2002, 57: 125−176.

[2] LEUZ A K, MÖNCH H, JOHNSON C A. Sorption of Sb(III) and Sb(V) to goethite: Influence on Sb(III) oxidation and mobilization [J].

Environmental Science Technology, 2006, 40: 7277−7282.

[3] MITSUNOBU S, TAKAHASHI Y, TERADA Y, SAKATA M. Antimony (V) incorporation into synthetic ferrihydrite goethite and natural iron oxyhydroxides [J]. Environmental Science Technology, 2010, 44: 3712−3718.

[4] NAVARRO P, ALGUACIL F J. Adsorption of antimony and arsenic from a copper electrorefining solution onto activated carbon [J]. Hydrometallurgy, 2002, 66 (6): 101−105.

[5] MITSUNOBU S, TAKAHASHI Y, SAKAI Y, INUMARU K. Interaction of synthetic sulfate green rust with antimony (V) [J]. Environmental Science Technology, 2009, 43: 318−323.

[6] OZCAN A, GOK O, OZCAN A. Adsorption of lead (II) ions onto 8-hydroxy quinoline immobilized bentonite [J]. Journal of Hazardous Materials, 2009, 161: 499−509.

[7] SULAYMON A H, ABID B A, AL-NAJAR J A. Removal of lead copper chromium and cobalt ions onto granular activated carbon in batch and fixed-bed adsorbers [J]. Chemical Engineering Journal, 2009, 155: 647−653.

[8] ESSINGTON M E, STEWART M A. Influence of temperature and pH on antimonate adsorption by gibbsite, goethite, and kaolinite [J]. Soil Science, 2015, 180(2): 54−66.

[9] RAKSHIT S, SARKAR D, PUNAMIYA P, DATTA R. Antimony sorption at gibbsite–water interface [J]. Chemosphere, 2011, 84: 480−483.

[10] TARGAN E, TIRTOM V N, AKKUŞ B. Removal of antimony (III) from aqueous solution by using grey and red erzurum clay and application to the gediz river sample [J]. IRSN Analytical Chemistry, 2013, 2013(6): 1−8.

[11] XU Wei, WANG Hong-jie, LIU Rui-ping, ZHAO Xu, QU Jiu-hui. The mechanism of antimony(III) removal and its reactions on the surfaces of Fe−Mn binary oxide [J]. Journal of Colloid Interface Science, 2011, 363: 320−326.

[12] GUO Xue-jun, WU Zhi-jun , HE Meng-chang. Removal of antimony (V) and antimony (III) from drinking water by coagulation-flocculation-sedimentation (CFS) [J]. Water Research, 2009, 43: 4327−4335.

[13] XIAO Fa-xin, CAO Dao, MAO Jian-wei, SHEN Xiao-Ni, REN Feng-zhang. Role of trivalent antimony in the removal of As, Sb, and Bi impurities from copper electrolytes [J]. International Journal of Minerals, Metallurgy, and Materials, 2013, 20: 9−16.

[14] FENG Ji-yun, HU Xi-jun, YUE Po Lock. Novel bentonite clay-based Fe-nanocomposite as a heterogeneous catalyst for photo-Fenton discoloration and mineralization of Orange II [J]. Environment Science Technolog, 2004, 1(38): 269−275.

[15] HASHEMIAN S. Removal of acid Red 151 from water by adsorption onto nano-composite $MnFe_2O_4$/kaolin [J]. Main Group Chemistry, 2011, 10: 105−114.

[16] HASHEMIAN S. Study of adsorption of acid dye from aqueous solutions using bentonite [J]. Main Group Chemistry, 2007, 6: 97−107.

[17] YAVUZ Ö, ALTUNKAYNAK Y, GUZEL F. Removal of copper, nickel, cobalt and manganese from aqueous solution by kaolinite [J]. Water Research, 2003, 37(4): 948−952.

[18] XI Jian-hong, HE Meng-chang, LIN Chun-ye. Adsorption of antimony (III) and antimony(V) on bentonite: Kinetics, thermodynamics and anion competition [J]. Micro Chemical Journal, 2011, 97: 85−91.

[19] XI Jian-hong, HE Meng-chang, LIN Chun-ye. Adsorption of antimony (V) on kaolinite as a function of pH, ionic strength and humic acid [J]. Environmental Earth Science, 2010, 60: 715−722.

[20] HASHEMIAN S, SADEGHI B, SALEHIFAR H, SALARI K, MOZAFARI F. Adsorption of disperse of yellow 42 onto bentonite and organo-modified bentonite by tetra butyl ammonium iodide (B-TBAI) [J]. Polish Journal Environmental Study, 2013, 22(5): 11−18.

[21] HASHEMIAN S, SHAHEDI M R. Novel Ag/kaolin nano composite as adsorbent for removal of acid cyanine 5R from aqueous solution [J]. Journal of Chemistry, 2013, 2013(2): 1−7.

[22] STANLEY J L. Am. Inst. industrial minerals and rock [M]. 5th ed. New York: Mining Engineers, 1983.

[23] YILMAZ I. Relationships between liquid limit, cation exchange capacity, and swelling potentials of clayey soils [J]. Eurasian Soil Science, 2004, 37(5): 506−512.

[24] ODOM I E. Smectite clay minerals: Properties and uses [J]. Philosophical Transactions of the Royal Society A: Mathematical Physical and Engineering Sciences, 1984, 311(1517): 391−409.

[25] HU Kun-hong, ZHAO Di-fang, LIU Jun-sheng. Synthesis of nano-MoS_2/bentonite composite and its application for removal of organic dye [J]. Transactions of Nonferrous Metals Society of China, 2012, 22(10): 2484−2490

[26] CHEN Yong-gui, HE Yong, YE Wei-min, SUI Wang-hua, XIAO Min-min. Effect of shaking time, ionic strength, temperature and pH value on desorption of Cr(III) adsorbed onto GMZ bentonite [J]. Transactions of Nonferrous Metals Society of China, 2013, 23(11): 3482−3489.

[27] MUBARAK H, CHAI Li-Yuan, MIRZA N, YANG Zhi-Hui, PERVEZ A, TARIQ M, SHAHEEN S, MAHMOOD Q. Antimony (Sb) pollution and removal techniques – critical assessment of technologies [J]. Toxicological and Environmental Chemistry, 2015, 97(10): 1296−1318.

[28] LUO Jin-ming, LUO Xu-biao, CRITTENDEN J, QU Jiu-hui, BAI Yao-hui, PENG Yue, LI Jun-hua. Removal of antimonite (Sb(III)) and antimonate (Sb(V)) from aqueous solution using carbon nanofibers that are decorated with zirconium oxide (ZrO_2) [J]. Environmental Science and Technology, 2015 49(18): 11115−11124.

[29] WANG Li, WAN Chun-Li, ZHANG Yi, TAY Joo-Hwa. Mechanism of enhanced Sb(V) removal from aqueous solution using chemically modified aerobic granules [J]. Journal of Hazardous Materials, 2015, 284: 43−49.

[30] XI Jian-hong, HE Meng-chang. Removal of Sb(III) and Sb(V) from aqueous media by goethite [J]. Water Quality Research Journal of Canada, 2013, 48(3): 223−231.

[31] SARI A, ŞAHINOĞLU G, TÜZEN M. Antimony(III) adsorption from aqueous solution using raw perlite and Mn-modified perlite: Equilibrium, thermodynamic, and kinetic studies [J]. Industrial and Engineering Chemistry Research, 2012, 51(19): 6877−6886.

[32] XIAO Fa-xin, CAO Dao, MAO Jian-wei, SHEN Xiao-ni, REN Feng-zhang. Role of Sb(V) in removal of As, Sb and Bi impurities from copper electrolyte [J]. Transactions of Nonferrous Metals Society of China, 2014, 24(1): 271−278.

[33] BANERJEE S, SHARMA G C, DUBEY S, SHARMA Y C. Adsorption characteristics of a low cost activated carbon for the removal of Victoria blue from aqueous solutions [J]. Journal Material Environmental Science, 2015, 6(8): 2045−2052.

[34] LIU Lin, YUN Gao-zhang, PING Su-xiu, CHEN Xing, JIANG Li, MING Yao-ju. Adsorption removal of dyes from single and binary solutions using a cellulose-based bioadsorbent [J]. ACS Sustainable Chemical Engineering, 2015, 3(3): 432−442.

[35] VADIVELAN V, VASANTH K K. Equilibrium, kinetics, mechanism, and process design for the sorption of methylene blue onto rice husk [J]. Journal Colloid Interface Science, 2005, 286: 90−100.

[36] OLIVEIRA L C A, RIOS R V R A, FABRIS J D, SAPAG K, GARG V K, LAGO R M. Clay–iron oxide magnetic composites for the adsorption of contaminants in water [J]. Applied Clay Science, 2003, 22: 169−177.

[37] HARRIS R G, WELLS J D, JOHNSON B B. Selective adsorption of dyes and other organic molecules to kaolinite and oxide surfaces [J]. Coll Sur A: Phys Eng Asp, 2001, 180: 131−140.

[38] HARRIS R G, WELLS J D, JOHNSON B B. Selective adsorption of dyes and other organic molecules to kaolinite and oxide surfaces [J]. Colloids and Surfaces A: Physicochemical and Engineering Aspects, 2001,180(1−2): 131−140.

[39] WU Rong-cheng, QU Jiu-hui, CHEN Yong-sheng. Magnetic powder $MnO-Fe_2O_3$ composite — A novel material for the removal of azo-dye from water [J]. Water Research, 2005, 39: 630−638.

[40] ZHANG Gao-sheng, QU Jiu-hui, LIU Hui-juan, COOPER A T, WU Rong-cheng. $CuFe_2O_4$/activated carbon composite: A novel magnetic adsorbent for the removal of acid orange II and catalytic regeneration [J]. Chemosphere, 2007, 68: 1058−1066.

[41] BERGAY A F, THENG BKG, LAGALY G. Handbook of clay science [M]. Oxford, UK: Elsevier, 2006.

[42] LI Fang-fei, JIANG Yin-shan, XIA Mao-sheng, SUN Meng-meng , XUE Bing, REN Xue-hong. A novel mesoporous silica–clay composite and its thermal and hydrothermal stabilities [J]. Journal of Porous Materials, 2010, 17: 217−223.

[43] MCLACHLAN M A, MCCOMB D W, BERHANU S, JONES T S. Template directed synthesis of nanostructured phthalocyanine thin films [J]. Journal of Materials Chemistry, 2007, 17: 3773−3776.

[44] XI Jian-hong, HE Meng-chang, LIN Chun-ye. Adsorption of antimony (V) on kaolinite as a function of pH, ionic strength and humic acid [J]. Environmental Earth Science, 2010, 60: 715−722.

[45] ANIRUDHA R C T S. Chromium (VI) adsorption by sawdust: Kinetics and equilibrium [J]. Indian Journal of Chemical Technology, 1997, 4: 228−236.

[46] LAGERGREN S. About the theory of so-called adsorption of soluble substances [J]. Kungliga Svenska Vetenskapsakademiens. Handlingar, 1898, 24(4): 1−39.

[47] HO Y S, MCKAY G, WASE D A J, FOSTER C F. Study of the sorption of divalent metal ions on to peat [J]. Adsorption Science and Technology, 2000, 18: 639−650.

[48] POOTS V J P, MCKAY G, HEALY J J. Removal of basic dye from effluent using wood as an adsorbent [J]. Journal Water Pollution Control Federation, 1978, 50: 926− 935.

采用不同吸附剂从铜电解液中除锑

Katereh SALARI[1], Saeedeh HASHEMIAN[1], Mohammad Taghi BAEI[2]

1. Department of Chemistry, Islamic Azad University, Yazd Brunch, P. O. Box 89195-155, Yazd, Iran;
2. Department of Chemistry, Islamic Azad University, Azadshahr Branch,
Azadshahr, P. O. Box 49617-89985 Golestan, Iran

摘　要：采用不同吸附剂，如活性炭、膨润土、高岭土、树脂、沸石和白沙从铜电解液中去除 Sb(V)，得到不同吸附剂从铜电解液中去除锑(V)的吸附容量顺序为：白沙<阴离子型树脂<沸石<高岭土<活性炭<膨润土。利用 FTIR、XRF、 XRD、 SEM 和 BET 等手段对膨润土进行表征。结果表明：膨润土的比表面积为 95 m^2/g，粒度为 175 nm；最大去除锑(V)的最佳条件为接触时间 10 min、4 g 膨润土和温度 40 °C；膨润土吸附锑 (V)遵守伪二级动力学方程(R^2=0.996，k=9×10^{-5} g/(mg·min))。热力学结果显示，膨润土从铜电解液中吸附锑(V)是吸热和自发的过程(ΔG^{Θ}=−4806 kJ/(mol·K)，吸附数据与 Freundlich 和 Langmuir 等温线模型吻合。在铜电解液中膨润土具有最大的吸附锑(V)容量为 10000 mg/g，对于铜电解液中的 Zn，Co，Cu 和 Bi 的吸附很低且影响不大。

关键词：锑(V)；膨润土；铜电解液；吸附剂；去除

(Edited by Xiang-qun LI)